$\pi\pi$ Scattering Amplitude in the Low-Energy Region*

M. R. Pennington and S. D. Protopopescu
Lawrence Berkeley Laboratory, University of California, Berkeley, California 94720
(Received 12 July 1972)

Recent unambiguous experimental $\pi\pi$ phase shifts are shown to be consistent at least up to 850 MeV with crossing and analyticity requirements, using the rigorously provable integral equations of Roy. We compute the s- and p-wave phase shifts in the experimentally unknown region from threshold to 500 MeV. We find the scattering lengths $a_0^0 = 0.15 \pm 0.07$ and $a_0^2 = -0.053 \pm 0.028$. We also calculate the s-, p-, and d-wave amplitudes in the subthreshold region and show that the current-algebra predictions of Weinberg are strongly supported by the data. We consider some phenomenological models which are in agreement with the data and discuss why their predictions are similar to Weinberg's.

I. INTRODUCTION

Low-energy $\pi\pi$ interactions have been the subject of intense study for the past ten years. While experimental results have appeared somewhat slowly, a multitude of theoretical models for the low-energy $\pi\pi$ scattering amplitude have been constructed.[1] These models are based on varying combinations of such apparently differing criteria as duality,[2] current algebra,[3] and the experimental p-wave phase shift.[4] When combined with crossing, analyticity, and elastic unitarity requirements, very similar results are generally predicted for the near-threshold behavior of the s- and p-wave amplitudes. Although these results may be dependent on the parametrization used, the fact that such models do have much in common in the very-low-energy region has led to the idea that they all possess some basic underlying dynamical mechanism, which appears to be the on-mass-shell appearance of the Adler zero.[5,6]

The experimental situation, particularly with regard to the $I=0$ s-wave phase shift, has until now been greatly confused by ambiguities. However, recent high-statistics experiments indicate that the "down" solution is the correct one for this partial wave beyond the ρ-resonance region.[6-8] With this clarification of the experimental data from 500 MeV to 1 GeV, we are now in a position to check whether these data are consistent with crossing and analyticity properties, and also to compute the $\pi\pi$ scattering amplitude in the experimentally unknown region from $s=0$ to 500 MeV using a dispersion-theoretic approach. In particular we shall compute the s-, p-, and d-wave scattering lengths from the data.

New theoretical tools, provable in axiomatic field theory, are now available with which to tackle this problem. We shall use the integral equations derived by Roy[9,10] (and discussed in Sec. II) as a check on the experimental data up to 850 MeV and to illustrate that the "down" solution does give a consistent $I=0$ s-wave phase shift (Sec. III). In Sec. IV we shall also use Roy's equations to compute the s and p waves in the unphysical region, and the Froissart-Gribov representation to calculate the d waves below threshold. Our resulting amplitude satisfies all the hundreds of rigorous constraints that such amplitudes must satisfy.[11] Moreover it is in good agreement with Weinberg's predictions.[3] That this is so is a direct result of the on-mass-shell appearance of the Adler zero and of the empirical truth of the Kawarabayashi-Suzuki-Riazuddin-Fayyazuddin (KSRF) relation.[12] In Sec. V we discuss these relationships and compare our experimentally determined amplitude with various theoretical predictions, including Weinberg's. In Table I we tabulate our results for the s-, p-, and d-wave scattering lengths.

II. NOTATION; ROY'S EQUATIONS

A. Notation

We write the s-channel partial-wave expansion for the amplitudes $F^I(s,t,u)$, which have definite s-channel isospin I, as

$$F^I(s,t,u) = \sum_{l=0}^{\infty} \tfrac{1}{2}[1+(-1)^{l+I}](2l+1) f_l^I(s) \times P_l\left(1+\frac{2t}{s-4}\right), \tag{2.1}$$

where we have set the pion mass equal to unity. Each partial-wave amplitude, $f_l^I(s)$, has a phase shift $\delta_l^I(s)$ and an inelasticity parameter $\eta_l^I(s)$ defined by

$$f_l^I(s)=\frac{1}{2i}\left(\frac{s}{s-4}\right)^{1/2}(\eta_l^I e^{2i\delta_l^I}-1). \tag{2.2}$$

η_l^I is equal to unity when elastic unitarity holds. In principle this is true only for $s\in(4,16)$; however, in practice, because the 4π threshold is weak, the partial-wave amplitudes are elastic up to much higher energies. In Fig. 1 we give the δ_0^0 and δ_1^1 phase shifts and corresponding inelasticities as determined by the recent experiment of Alston-Garnjost *et al.*[7]

Finally we define the scattering lengths, a_l^I, by

$$a_l^I=\lim_{s\to 4}\frac{f_l^I(s)}{[\frac{1}{4}(s-4)]^l}. \tag{2.3}$$

With these conventions the optical theorem reads

$$A^I(s,0,4-s)\equiv \mathrm{Im}\,F^I(s,0,4-s)=\frac{[s(s-4)]^{1/2}}{16\pi}\sigma_{\mathrm{tot}}^I(s). \tag{2.4}$$

B. Roy's Equations

Using only assumptions provable in axiomatic field theory, Roy[9] has derived an exact set of equations for the partial-wave amplitudes expressed as integrals over the physical region absorptive parts. These equations, which embody both crossing and the analyticity of twice-subtracted dispersion relations, will be used as a consistency check on the experimental data and also to compute the partial-wave amplitudes in experimentally unknown regions.

These equations are derived by using crossing symmetry to reexpress the t-dependent subtraction functions of twice-subtracted fixed-t dispersion relations in terms of scattering lengths and integrals over the absorptive parts. Projecting out the partial waves, one obtains an equation of the following form:

$$f_l^I(s)=\text{s.t.}+\sum_{I'=0}^{2}\sum_{l'=0}^{\infty}(2l'+1)\int_4^\infty dy\, G_{l,l'}^{I,I'}(s,y)\,\mathrm{Im}f_{l'}^{I'}(y), \tag{2.5}$$

where s.t. are the subtraction terms present only in the s and p waves. Such an equation is valid for

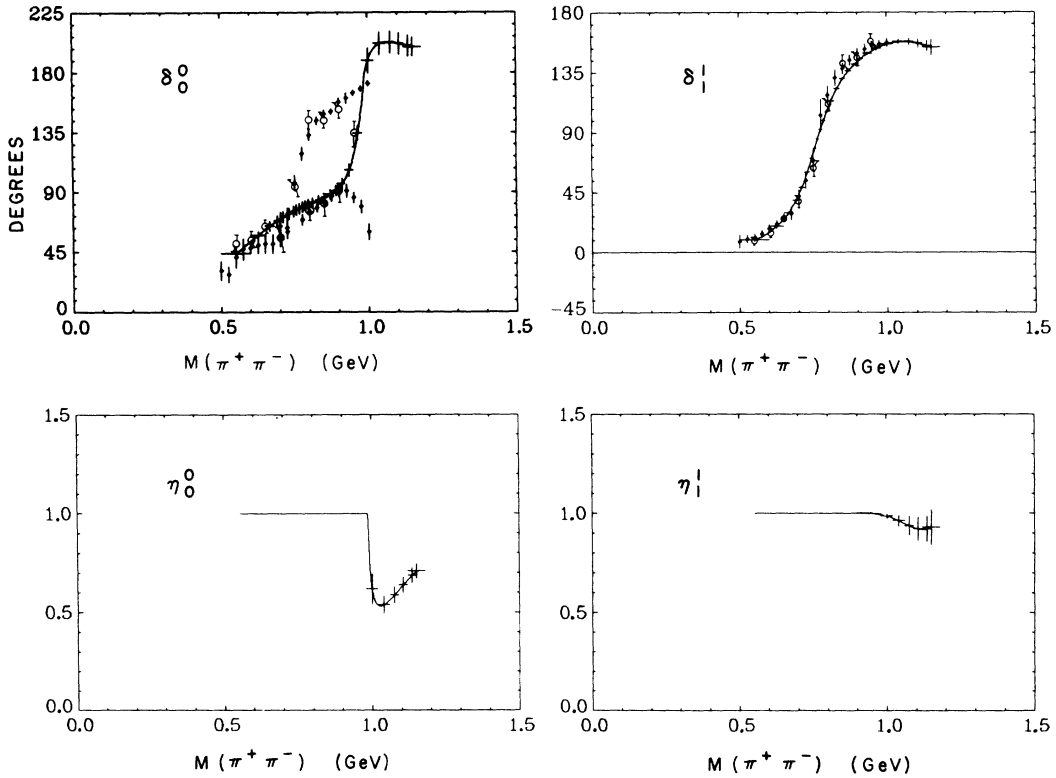

FIG. 1. The phases and inelasticities of the $I=0$ s wave and the $I=1$ p wave from Ref. 7. The vertical lines indicate the calculated errors at a given mass. These errors are purely statistical (Ref. 7). The plotted points correspond to the elastic "down" and "up" solutions of Baton *et al.* (Ref. 8). The open circles are the results of Baillon *et al.* (Ref. 8).

$$-4 \leq s \leq 60 . \tag{2.6}$$

The functions G are in general rather complicated. They are given in Ref. 10. However, it will be useful to write Eq. (2.5) in more detail for the s and p waves so as to display the subtractions terms and the explicit dependence on the imaginary parts of these partial waves[10]:

$$\begin{aligned} f_0^0(s) = a_0^0 + \tfrac{1}{12}(2a_0^0 - 5a_0^2)(s-4) + \frac{s-4}{\pi}\int_4^\infty dy \frac{\operatorname{Im} f_0^0(y)}{(y-s)(y-4)} \\ + \frac{2}{\pi}\int_4^\infty \frac{dy}{y}[Q_1(z) - Q_0(z)][\tfrac{1}{3}\operatorname{Im} f_0^0(y) + 3x \operatorname{Im} f_1^1(y) + \tfrac{5}{3}\operatorname{Im} f_0^2(y)] \\ - \frac{1}{3}\frac{s-4}{\pi}\int_4^\infty \frac{dy}{y(y-4)}[2\operatorname{Im} f_0^0(y) - 9\operatorname{Im} f_1^1(y) - 5\operatorname{Im} f_0^2(y)] + \sum_{l'=0}^{2}\sum_{l'=2}^{\infty}(2l'+1)\int_4^\infty dy\, G_{0,0}^{l',l'}(s,y)\operatorname{Im} f_{l'}^{l'}(y), \end{aligned} \tag{2.7}$$

$$\begin{aligned} f_0^2(s) = a_0^2 - \tfrac{1}{24}(2a_0^0 - 5a_0^2)(s-4) + \frac{s-4}{\pi}\int_4^\infty dy \frac{\operatorname{Im} f_0^2(y)}{(y-s)(y-4)} \\ + \frac{2}{\pi}\int_4^\infty \frac{dy}{y}[Q_1(z) - Q_0(z)][\tfrac{1}{3}\operatorname{Im} f_0^0(y) - \tfrac{3}{2}x \operatorname{Im} f_1^1(y) + \tfrac{1}{6}\operatorname{Im} f_0^2(y)] \\ + \frac{1}{6}\frac{s-4}{\pi}\int_4^\infty \frac{dy}{y(y-4)}[2\operatorname{Im} f_0^0(y) - 9\operatorname{Im} f_1^1(y) - 5\operatorname{Im} f_0^2(y)] + \sum_{l'=0}^{2}\sum_{l'=2}^{\infty}(2l'+1)\int_4^\infty dy\, G_{0,2}^{l',l'}(s,y)\operatorname{Im} f_{l'}^{l'}(y), \end{aligned} \tag{2.8}$$

$$\begin{aligned} f_1^1(s) = \tfrac{1}{72}(2a_0^0 - 5a_0^2)(s-4) + \frac{s-4}{\pi}\int_4^\infty \frac{dy \operatorname{Im} f_1^1(y)}{(y-s)(y-4)} \\ + \frac{4}{\pi(s-4)}\int_4^\infty dy\, Q_1(z)[\tfrac{1}{3}\operatorname{Im} f_0^0(y) + \tfrac{3}{2}x \operatorname{Im} f_1^1(y) - \tfrac{5}{6}\operatorname{Im} f_0^2(y)] \\ - \frac{1}{18}\frac{s-4}{\pi}\int_4^\infty \frac{dy}{y(y-4)}[2\operatorname{Im} f_0^0(y) + 27\operatorname{Im} f_1^1(y) - 5\operatorname{Im} f_0^2(y)] + \sum_{l'=0}^{2}\sum_{l'=2}^{\infty}(2l'+1)\int_4^\infty dy\, G_{1,1}^{l',l'}(s,y)\operatorname{Im} f_{l'}^{l'}(y), \end{aligned} \tag{2.9}$$

where

$$x = 1 + \frac{2s}{y-4}, \quad z = 1 + \frac{2y}{s-4} .$$

In the next section we will discuss how these equations are used and in particular how we determine the all-important subtraction terms.

III. EXPERIMENTAL DATA AND ROY'S EQUATIONS

A. Introduction

We have reliable experimental data for the s- and p-wave amplitudes only in a limited energy region, from 500 to 1050 MeV. We shall use for the $I=0$ s wave and the $I=1$ p wave the data from Ref. 7, which are illustrated in Fig. 1. For the $I=2$ s wave we use the results of Baton *et al.*[8] Since Roy's equations, (2.5), require knowledge of the imaginary parts of the partial-wave amplitudes from threshold to infinity, we must discuss how we are going to approximate the contributions from other energy regions and other partial waves.

As noted by Basdevant, Le Guillou, and Navelet[10] the partial waves with $l \geq 2$ contribute most for $y \leq \frac{1}{2}(s-4)$. That is, the higher partial waves contribute most for larger values of s. However, only the near-threshold behavior of these waves is at all important. The required behavior of these imaginary parts can be estimated from the real parts using unitarity, i.e., $\operatorname{Im} f_l \simeq [(s-4)/s]^{1/2} \times (\operatorname{Re} f_l)^2$, and the real parts can be estimated using a scattering-length approximation. The scattering lengths can, in turn, be computed from the appropriate Froissart-Gribov representation for the

$l \geq 2$ partial waves:

$$f_l^I(s) = \frac{4}{\pi(s-4)} \int_4^\infty dt \sum_{I'} C_{II'} A^{I'}(t,s) Q_l\left(1+\frac{2t}{s-4}\right), \tag{3.1}$$

where $C_{II'}$ is the s-t isospin crossing matrix, and where the t-channel absorptive part $A^{I'}(t,s)$ can be expressed in terms of their partial waves, $\mathrm{Im} f_l^{I'}(t)$, for $-28 \leq s \leq 4$.

It is appropriate to make a comment here for later use. While the Froissart-Gribov representation, Eq. (3.1), can only be proved to be valid for the $l \geq 2$ partial waves, because of the need to comply with the Froissart bound by using twice-subtracted dispersion relations, in practice the Froissart-Gribov representation may hold for lower partial waves. If one believes in some sort of Regge asymptotics then a ρ-trajectory function, $\alpha_\rho(s)$, with $\alpha_\rho(s) < 1$ for $s \leq 4$, guarantees that such a representation exists for the partial-wave amplitude, $f_1^1(s)$.[13] While this is a very useful relation which we make use of later, the fact that the $I=2$ s wave may also satisfy a Froissart-Gribov relation is much less useful for our purposes, because of the slower convergence of the integrand. Therefore we do not utilize this possible phenomenological result for the $I=2$ s-wave amplitude.[14]

To approximate the imaginary parts of the amplitude beyond $y=53$, where the reliable data end, we note that for large y, $G \sim y^{-3}$. Therefore, the integration over y in Eq. (2.5) converges very rapidly, damping down the contribution from the Regge region. Although for $s > 12$ (i.e., $\sqrt{s} \gtrsim 480$ MeV) this intermediate- and high-energy contribution cannot be neglected, our results are not particularly sensitive to the details of the Regge parametrization used in Roy's equation until s is much larger (e.g., $s \simeq 36$, $\sqrt{s} \simeq 840$ MeV). We include the f_0 resonance in the intermediate-energy region from $y=53$ up to $y = \frac{1}{2}(m_f^2 + m_g^2) \simeq 115$ and assume that beyond that energy the imaginary parts of the amplitude are given by simple Pomeranchukon and ρ exchange. We estimate the contribution of the background to the intermediate-energy term by appealing to the Freund-Harari conjecture and assume that the nonresonant background is given by the Pomeranchukon-exchange amplitude [Eq. (3.5)]. These intermediate- and higher-energy terms contribute a polynomial in s to Eq. (2.5). For simplicity, we only attempt to estimate those high-energy contributions up to a quadratic in s. This enables us to make a rather crude estimate with some degree of certainty since a more detailed Regge parametrization only affects the cubic and higher terms in s.

For the f_0 amplitude we use a modified Breit-Wigner form given by[14]

$$f_2^0(y) = \left(\frac{m_f^2}{y-4}\right)^{1/2} \frac{m_f \Gamma_f(y)}{m_f^2 - y - i m_f \Gamma_f(y)}, \tag{3.2}$$

where

$$\Gamma_f(y) = \gamma_f \left(\frac{y-4}{m_f^2-4}\right)^{1/2} \frac{P_2(1+2m_\rho^2/(m_f^2-4))}{P_2(1+2m_\rho^2/(y-4))}. \tag{3.3}$$

m_f and γ_f are the resonance mass and width, which we take to be (assuming the resonance is purely elastic)

$$m_f = 1269 \text{ MeV}, \quad \gamma_f = 156 \text{ MeV}.$$

For the Pomeranchukon term we take

$$A^{I_t=0}(y,t) \simeq \beta_P(t) y^{\alpha_P(t)}, \tag{3.4}$$

where

$$\beta_P(0) = \frac{3}{32\pi} \sigma_{\text{tot}}^{\pi\pi}. \tag{3.5}$$

We make the rough approximation

$$\begin{aligned} &\alpha_P(t) = 1, \\ &\beta_P(t) = \beta_P(0) e^{bt/2}. \end{aligned} \tag{3.6}$$

In agreement with factorization and the analysis of Caso *et al.*,[15] we take

$$\sigma_{\text{tot}}^{\pi\pi} = 20 \pm 10 \text{ mb},$$

$$b = 8 \pm 3 \ (\text{GeV}/c)^{-2}.$$

Such a large error takes into account not only the crude parametrization we have used but also the small contribution from the ρ exchange.

Substituting Eq. (3.2) for the d wave and Eq. (3.1) for $l > 2$, together with the partial-wave projection of Eq. (3.4), into Eqs. (2.7)–(2.9), we find that the lowest-order contributions of the f_0 resonance and Regge terms to $f_0^0(s)$, $f_1^1(s)$, and $f_0^2(s)$ are

$$f_0^0(s;\text{HE}) = (13 \pm 5) \times 10^{-5} (s^2 - 16), \tag{3.7}$$

$$f_0^2(s;\text{HE}) = (13 \pm 6) \times 10^{-5} s(s-4), \tag{3.8}$$

$$f_1^1(s;\text{HE}) = (3.0 \pm 1.5) \times 10^{-5} s(s-4), \tag{3.9}$$

where HE denotes high energy. These forms are only true for $4 < s << 53$.

Of course, cubic and higher terms in s, which we neglect here, become increasingly important for larger s; however, the quadratic terms given above will be sufficient for our purposes.

We now turn to the most important problem of how to parametrize the imaginary parts of the s and p waves from threshold to 500 MeV. This is the subject of the next section.

B. Determination of the Subtraction Terms

The determination of the subtraction terms in Eqs. (2.7)–(2.9) is intimately related to how we deal with the s and p waves from threshold to where the data begin. The method is to use Roy's equations together with unitarity to obtain a self-consistent set of real and imaginary parts for the partial waves in this experimentally unknown region. For each such self-consistent solution there will be a given value for the subtraction terms. We further require that these subtraction terms give, via Roy's equations, real parts for the partial-wave amplitudes which agree with the data beyond 500 MeV.

We start these attempts to find consistent solutions by computing the p-wave scattering length, a_1^1, by two different methods which we now describe.

(a) First we compute a_1^1 from the Froissart-Gribov representation [Eq. (3.1)], which we assume exists as discussed in Sec. III A. Evaluated at $s=4$ we have

$$a_1^1=\frac{4}{3\pi}\int_4^\infty \frac{dy}{y^2}\left[\tfrac{1}{3}A^0(y,4)+\tfrac{1}{2}A^1(y,4)-\tfrac{5}{6}A^2(y,4)\right]. \tag{3.10}$$

We divide this integral into four distinct regions, which we now discuss one by one. Region (i), from $y=4$ to 13, is where we want to determine the s- and p-wave amplitudes, and so will be considered later. Region (ii), from $y=13$ to 53, is where we have the data. We integrate this by using a fit to the data determined in Ref. 7, which includes the $I=2$ s-wave data of Baton *et al.*[8] To estimate the errors involved in this, we also integrate a second fit which passes through the extreme ends of the error bars.[7] This should give our integrals a realistic uncertainty.

Region (iii) is the intermediate-energy or resonance region. In this we include the f_0 resonance and use the form of the f_0 amplitude given in Eq. (3.2). We integrate this from threshold to where Regge asymptotics begins. As before we assume that Regge behavior is valid for a value of y halfway between the f_0 and g resonances, i.e., $y\simeq 115$.

Region (iv) is the Regge region ($y\geq 115$). Because the integrand of Eq. (3.10) converges more slowly by one explicit power of y than Roy's equations, the high-energy contribution is relatively more important. This high-energy term is controlled by ρ exchange, for which we require a more detailed parametrization because of the slower convergence. We follow Le Guillou, Morel, and Navelet[4] and use

$$A^{I_s=1}(y,s=4)=\beta_\rho \sin\pi\alpha_\rho(4)\left(\frac{y}{y_0}\right)^{\alpha_\rho(4)}\Gamma(1-\alpha_\rho(4)), \tag{3.11}$$

where

$$\alpha_\rho(4)=0.5,\quad 30\leq y_0\leq 50, \tag{3.12}$$

$$\beta_\rho=\frac{3m_\rho{}^2\Gamma_\rho\alpha'_\rho y_0}{(m_\rho{}^2-4)^{3/2}},\quad \alpha'_\rho=\frac{1-\alpha_\rho(4)}{(m_\rho{}^2-4)}.$$

We have used the fact that the small variation in $\alpha_\rho(s)$ between $s=0$ and 4 has negligible effect on our calculation to approximate $\alpha_\rho(4)$ by $\frac{1}{2}$. The residue parameter β has been determined by extrapolation to the ρ mass. The parameter y_0 takes into account the variation of the residue function from $s=4$ to $s=m_\rho{}^2$.[16]

The intermediate- and high-energy contributions to Eq. (3.10) are numerically

$$a_1^1(\mathrm{IE})=(3.38\pm 0.34)\times 10^{-3},$$
$$a_1^1(\mathrm{HE})=(9.72\pm 1.30)\times 10^{-3}. \tag{3.13}$$

We then have

$$a_1^1=\frac{4}{3\pi}\int_4^{53}\frac{dy}{y^2}\left[\tfrac{1}{3}\,\mathrm{Im}f_0^0(y)+\tfrac{3}{2}\left(\frac{y+4}{y-4}\right)\mathrm{Im}f_1^1(y)-\tfrac{5}{6}\,\mathrm{Im}f_0^2(y)\right]+(1.31\pm 0.16)\times 10^{-2}. \tag{3.14}$$

To compute the integral from $y=4$ to 53 we use the fit of Ref. 7 extrapolated all the way down to threshold (this fit will be referred to as SCAT). This will give us a starting value for a_1^1.

(b) Given a value for a_1^1 we can compute the subtraction constant $2a_0^0-5a_0^2$ by using a sum rule which was first obtained by Wanders using the Mandelstam representation,[13] but which follows more generally from Roy's equation. Consider Eq. (2.9) and divide by $(s-4)$. Using the definition of the scattering lengths, Eq. (2.3), and setting $s=4$ we obtain

$$2a_0^0-5a_0^2-18a_1^1=\frac{16}{\pi}\int_4^\infty\frac{dy}{y^2(y-4)}\left[2A^0(y,0)-5A^2(y,0)-\frac{3(3y-4)}{(y-4)}A^1(y,0)\right]. \tag{3.15}$$

We divide the integral into two parts. The one with $y>53$ is estimated from Eq. (3.9) to contribute $-(8.6\pm4.3)\times10^{-3}$. The integral from $y=4$ to 53 is evaluated using SCAT. This gives us a first value for $2a_0^0-5a_0^2-18a_1^1$, which together with our initial evaluation of a_1^1 provides us with a starting value of the subtraction constant, $2a_0^0-5a_0^2$.

(c) We next choose a value for the second subtraction constant, a_0^0, at random in the range $(0,0.4)$. Using this a_0^0 and our first value for $2a_0^0-5a_0^2$, together with SCAT to calculate the integrals, we can compute the real parts of f_0^0, f_1^1, and f_0^2 as functions of s from threshold upwards. Next we use unitarity to compute the corresponding imaginary parts. Since in SCAT the imaginary parts below 500 MeV have been obtained by extrapolating a fit and are not experimentally determined quantities, we replace these imaginary parts in SCAT below 500 MeV by those obtained from Roy's equations, via unitarity. With these new estimates of the imaginary parts we repeat the cycle. We recompute a_1^1 and $2a_0^0-5a_0^2$ from Eqs. (3.14) and (3.15). Then keeping our value of a_0^0 fixed we recalculate the real and imaginary parts of the partial-wave amplitudes. This is repeated until no change is observed from one iteration to the next. For this procedure to converge after a reasonable number of iterations (i.e., less than 50) with $a_0^0>0.2$ we had to assume that the data were known down to 480 MeV (rather than 500 MeV). This was because for larger values of a_0^0 the real part of the $I=0$ s wave, computed from Roy's equations, may violate the unitarity bound below 500 MeV during the iteration procedure. Since the imaginary parts are not properly defined for such real parts (i.e., when $[(s-4)/s]^{1/2}\times\mathrm{Re}f_0^0(s)=\frac{1}{2}\sin2\delta_0^0(s)>\frac{1}{2}$), this can produce instabilities in our iteration procedure. By using the fit given by SCAT down to 480 MeV, for the larger values of $a_0^0\in(0,0.4)$, we were always able to obtain convergence in 8–20 iterations. Thus for a given value of $a_0^0\in(0,0.4)$ we obtain a self-consistent set of real and imaginary parts for the s- and p-wave amplitudes below 500 MeV. We now want to choose those values for a_0^0 which give real and imaginary parts for these partial waves in agreement with the data beyond 500 MeV. Since the energy region from 520 to 700 MeV (i.e., $s=14$–26) depends most sensitively on the subtraction terms, we shall only use the data in this range to define an *"ad hoc"* χ^2. We define this χ^2 in the following way:

$$\chi^2=\int_{14}^{26}ds\left[\frac{\mathrm{Re}f_e(s)-\mathrm{Re}f_c(s)}{\sigma(s)}\right]^2, \tag{3.16}$$

where $\mathrm{Re}f_e(s)$, $\mathrm{Re}f_c(s)$ are the experimental and computed real parts, respectively, of the partial-wave amplitudes; σ^2 is the sum of the squares of the experimental and computed errors in these real parts. The computed error includes the uncertainty in the high-energy contributions of Eqs. (3.7)–(3.9) and Eqs. (3.14), (3.15) as well as the errors in the integrals over the data.

For all our self-consistent solutions with $a_0^0\in(0,0.4)$ we can compute the values χ^2 for each s and p wave. We find that this χ^2 for the $I=1$ p wave depends little on the value of a_0^0. This is mainly because a_1^1 and $2a_0^0-5a_0^2$ change by at most 25% for $a_0^0\in(0,0.4)$. For the $I=2$ s wave the experimental errors[8] are too large for us to be able to use χ^2 in a meaningful way. However, in contrast, we find that χ^2 for the $I=0$ s wave has a very sharp minimum as a function of a_0^0, which is shown in Fig. 2. We therefore use this to define the central value for this scattering length, and so obtain

$$a_0^0=0.152\,.$$

However, our χ^2 is not a meaningful quantity with which to define the error on this parameter; i.e., it is not directly related to the number of degrees of freedom, which are not well defined in this case. The experimental points used[7] were obtained in an energy-dependent fit; therefore one cannot treat each point as statistically independent. What we do instead to define the extreme values of a_0^0 is to observe where the bands of experimental and computed values for the $\mathrm{Re}f_0^0(s)$ barely overlap in the region from 500 to 700 MeV. (See Fig. 3.) This criterion gives

$$a_0^0=0.15\pm0.07\,. \tag{3.17}$$

As noted before, the agreement we obtain for $\mathrm{Re}f_1^1(s)$ is little altered by the value of a_0^0, since this real part depends most on a_1^1 and $2a_0^0-5a_0^2$.

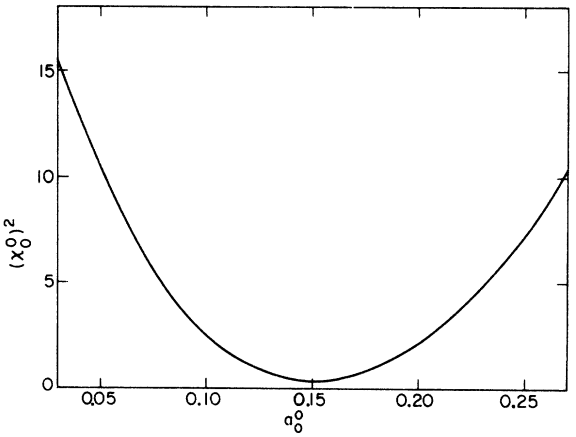

FIG. 2. A plot of $(\chi_0^0)^2$, defined by Eq. (3.16), versus a_0^0.

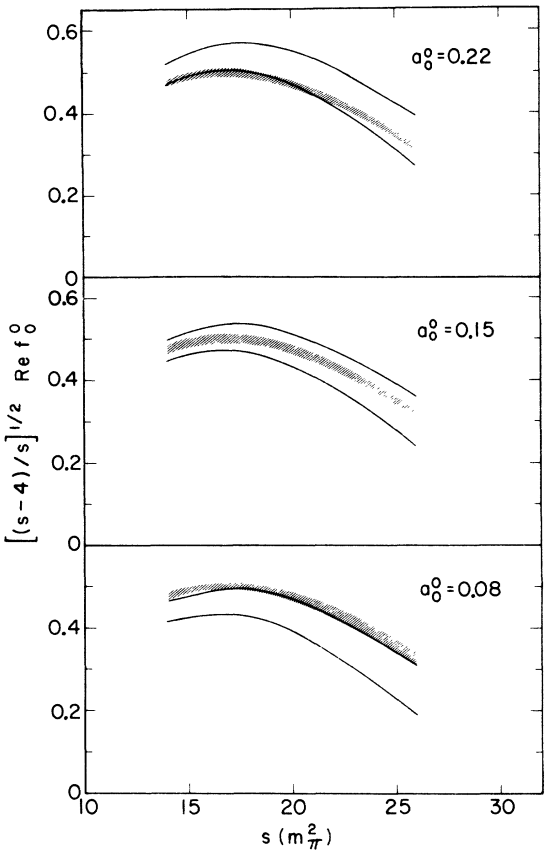

FIG. 3. The cross-hatched band contains the experimental values of $[(s-4)/s]^{1/2}\mathrm{Re}f_0^0(s)$ from Ref. 7. The solid lines indicate the range of values for the same quantity calculated using Roy's equations with a fixed value of a_0^0 ($a_0^0 = 0.08$, 0.15, and 0.22 are shown).

For a_0^0 in the range given by Eq. (3.17) we find

$$a_1^1 = 0.0357 \pm 0.0020 \tag{3.18}$$

and

$$2a_0^0 - 5a_0^2 = 0.569 \pm 0.040\,. \tag{3.19}$$

These values are to be compared with Weinberg's prediction[3]:

$$a_0^0 = 0.195, \quad 2a_0^0 - 5a_0^2 = 0.67 \quad \text{if } f_\pi = 83 \text{ MeV}$$
(the Goldberger-Treiman value);
$$a_0^0 = 0.150, \quad 2a_0^0 - 5a_0^2 = 0.52 \quad \text{if } f_\pi = 95 \text{ MeV}$$
(the experimental value). (3.20)

From our determination of a_0^0 and $2a_0^0 - 5a_0^2$ we obtain for the $I=2$ s-wave scattering length the value

$$a_0^2 = -0.053 \pm 0.028\,, \tag{3.21}$$

which gives the ratio

$$\frac{a_0^0}{a_0^2} = -2.9 \pm 2.0\,, \tag{3.22}$$

to be compared with the independent experimental determinations of this ratio,[17] -3.1 ± 1.1, and with Weinberg's prediction of -3.5. All our results for the scattering lengths are summarized in Table I for easier reference.[18]

C. Are the Data Consistent with Crossing and Analyticity Properties?

Knowing the subtraction terms, we can now use Eqs. (2.7)–(2.9) to compute the real parts of the s- and p-wave amplitudes from threshold upwards. We, of course, already know that our computed results will agree with the data at least up to 700 MeV, but what happens beyond that energy?

The computed bands for $\delta_0^0(s)$, $\delta_0^2(s)$, and $\delta_1^1(s)$ are illustrated in Figs. 4 and 5 together with the data.[7,8] The bands reflect the uncertainties in our knowledge of a_0^0 and a_0^2, and of the lowest order high-energy corrections, as well as the experimental errors on the imaginary parts. As can be seen, we have remarkable agreement up to $\sqrt{s} \simeq 850$ MeV, particularly for the $I=1$ p wave, for which there is less uncertainty in the data. The deviation at higher energies is not surprising since we have only included estimates for the quadratic terms in s from the high-energy contributions, and this is clearly unrealistic for energies closer to 1 GeV than threshold. Nevertheless we see that the "down" solution for δ_0^0, beyond 720 MeV, is completely consistent with the general theoretical properties built into Roy's equations.[19]

We have also used the same procedure as described in Sec. IIIB replacing the "down" solution for δ_0^0 beyond 720 MeV by an "up" solution. Although self-consistent real and imaginary parts can be obtained up to 700 MeV, we have been unable to produce a δ_0^0 phase shift which rises rapidly enough in the ρ-resonance region. A more systematic study of this, together with a discussion of

TABLE I. Our results for the s-, p-, and d-wave scattering lengths.

a_l^I	Scattering-length values
a_0^0	0.15 ± 0.07
a_0^2	-0.053 ± 0.028
$2a_0^0 - 5a_0^2$	0.57 ± 0.04
a_1^1	0.036 ± 0.002
a_2^0	$(1.69 \pm 0.05) \times 10^{-3}$
a_2^2	$(0.7 \pm 3.0) \times 10^{-5}$

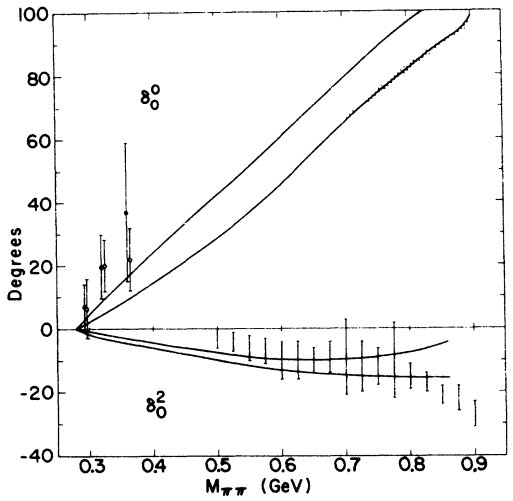

FIG. 4. The $I = 0$ and 2 s-wave phase shifts: The bands bordered by the solid lines are those computed from Eqs. (2.7) and (2.8). The cross-hatched band corresponds to the experimental results for δ_0^0 of Ref. 7, also shown in Fig. 1. The K_{e4} results of Ref. 20 are shown for comparison, where the open circles are the points fixed by their χ^2 fit, and the solid points are those determined by the Pais-Treiman method (Ref. 20). The data points for δ_0^2 are from Baton *et al.* (Ref. 8).

the intermediate-energy region, which includes the S^* and f_0 resonances, will be the subject of a forthcoming article.

Since the "down" solution for $\delta_0^0(s)$, beyond 700 MeV, is confirmed, we can have great confidence in our determination of the partial waves in the experimentally unknown region from threshold to 500 MeV. However, we should note that our values for $\delta_0^0 - \delta_1^1$, in the region 300–360 MeV, are not in complete agreement with those values obtained from K_{e4} results,[20] which are also shown in Fig. 4, but within their large errors they are not inconsistent. We now proceed to calculate the s-, p-, and d-wave amplitudes in the unphysical region from threshold to pseudothreshold.

IV. PARTIAL WAVES IN THE UNPHYSICAL REGION

A. Results

In computing the s, p, and d waves below threshold we shall neglect both the contribution from the higher partial waves up to 1 GeV and that of the high-energy term. While the contribution from the higher partial waves is definitely negligible, the neglect of the high-energy term will affect our results slightly. For example, the values of the partial waves at $s = 0$ will change by a few percent, but since we have a 50% uncertainty in the s-wave scattering lengths this seems justified.

However, more than this, just computing f_0^0, f_1^1, f_0^2, f_2^0, and f_2^2 from the imaginary parts of the s and p waves ensures that crossing symmetry is satisfied, since with $\mathrm{Im} f_l^I(s) = 0$, for $l \geq 2$, the supplementary crossing conditions of Roy are trivially satisfied.[9,21] In fact all known crossing, analyticity, and positivity constraints on the s, p, and d waves below threshold will be satisfied in this way.[11]

The results of using Eqs. (2.7)–(2.9) to compute f_0^0, f_1^1, and f_0^2 are illustrated in Fig. 6; no errors have been assigned although they are primarily just those already given to the appropriate scattering length, i.e., the uncertainty in $f_0^0(s)$ is just ± 0.07, while in $f_1^1(s)$ it is $\pm 0.002(s-4)$. The $\pi^0\pi^0$ s wave, $f_0^{00}(s) = \frac{1}{3}(f_0^0 + 2f_0^2)$, which is of particular interest with regard to the rigorous constraints discussed in Ref. 11, is shown in Fig. 7. The d wave f_2^0 and the $\pi^0\pi^0$ combination $f_2^{00}(s)$ were calculated from the Froissart-Gribov representation of Eq. (3.1) and are depicted in Fig. 8. Although the slope of the $\pi^0\pi^0$ d wave can be rigorously proved to be negative from $s = 4$ down to at best $s = \frac{4}{3}$,[22] we see that our d wave has negative slope for all $s \in (0, 4)$ just as suggested by Martin.[23] This means that the $\pi^0\pi^0$ d wave has only one second-sheet pole for $s \in (0, 4)$.[22,23]

The values we obtain for the d-wave scattering lengths are

$$a_2^0 = (1.69 \pm 0.05) \times 10^{-3}, \qquad a_2^2 = (0.7 \pm 3.0) \times 10^{-5}. \tag{4.1}$$

These quantities include contributions from high-

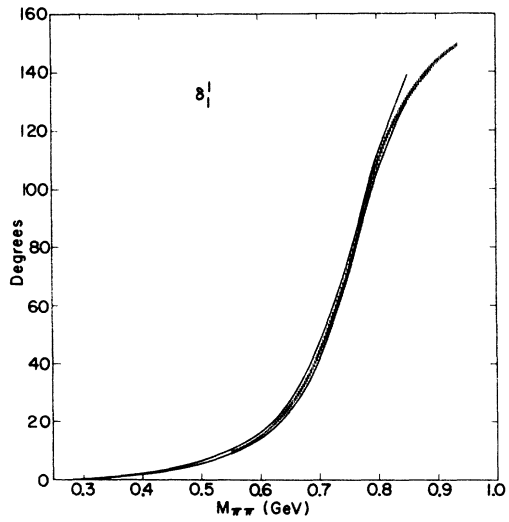

FIG. 5. The $I = 1$ p-wave phase shift: The band bordered by solid lines is that computed from Eq. (2.9). The cross-hatched band corresponds to the experimental results of Ref. 7, also shown in Fig. 1.

energy terms, and their errors are again estimated by the method discussed in Sec. IIIB. We note that the exotic d-wave scattering length is at least two orders of magnitude less than the corresponding $I=0$ scattering length, giving support to the assumptions of Ref. 4. We also remark that the value for the $I=0$ d-wave scattering length of Eq. (4.1) is very close to that given by assuming that the threshold behavior for this partial-wave amplitude is dominated by the tail of the f_0 resonance and setting $\gamma=4$ in Eq. (3.2).

B. Subthreshold Zeros, the Adler Zero, and the ρ Resonance

While including the high-energy contributions which we have neglected would slightly alter our results, the form of our s, p, and d waves, shown in Figs. 6–8, must be very close to the true situation within the errors assigned to the scattering lengths (Table I).

A most important point to note is that the $I=0$ and 2 s-wave amplitudes have zeros at $s=s_0=1.10$ and $s=s_2=1.49$, respectively, with $a_0^0=0.15$ and $a_0^2=-0.053$. These positions give $4s_0+5s_2=11.9$. Changing the s-wave scattering lengths within their uncertainties will change the positions of the s-wave zeros, but since the relation (3.19) must still be satisfied, the positions of the s-wave zeros will continue to obey the condition

$$4s_0+5s_2\simeq 12\,. \tag{4.2}$$

Let us make a brief comment on this relationship, discussed in Ref. 6, which seems to have been the source of some confusion. In an exactly linear model where

$$f_0^0=2a(s-s_0),\qquad f_0^2=a(s_2-s)\,, \tag{4.3}$$

s_0 and s_2 satisfy Eq. (4.2) exactly just from crossing symmetry, regardless of the values of s_0 and s_2, which may in general of course be outside the region (0, 4). However, it is shown in Ref. 6 that if s_0 is roughly in the range (0.2, 1.5) and s_2 is related to s_0 by the approximate relation Eq. (4.2), then, assuming a simple quadratic off-mass-shell extrapolation, the on-mass-shell amplitude is consistent with the vanishing of the off-shell amplitude at or very close to the Adler point, $s=t=u=1$.[5] However, more important in this respect is the fact that the on-shell Chew-Mandelstam invariant amplitude,[24] $A(s,t,u)=\frac{1}{3}[F^0(s,t,u)-F^2(s,t,u)]$, has a line of zeros in the Mandelstam triangle, shown in Fig. 9, which is very much like that depicted in Fig. 1 of Ref. 6 as the on-shell appearance of the Adler zero. As discussed earlier in Ref. 25, the real-s, real-t projection of this complex zero continues smoothly into the physical region to become the Legendre zero of the ρ resonance. This is a very important point in linking current-algebra-based models and p-wave-dominant solutions to $\pi\pi$ scattering.

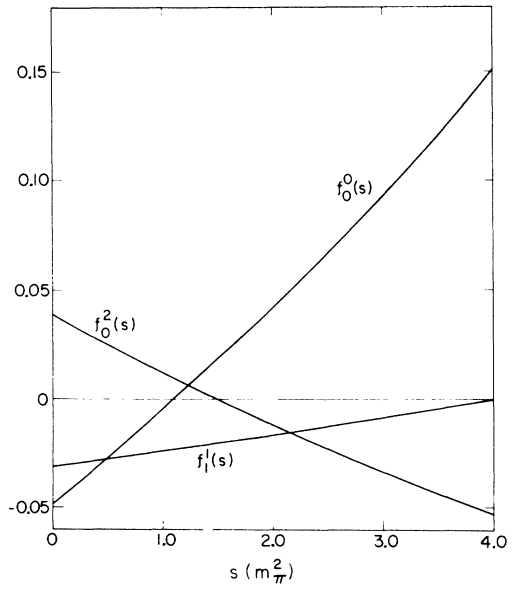

FIG. 6. The partial-wave amplitudes f_0^0, f_0^2, and f_1^1 below threshold from $s=0$ to 4, computed from Eqs. (2.7), (2.8), and (2.9), respectively, with scattering lengths of $a_0^0=0.15$, $a_0^2=-0.053$, and $a_1^1=0.0357$.

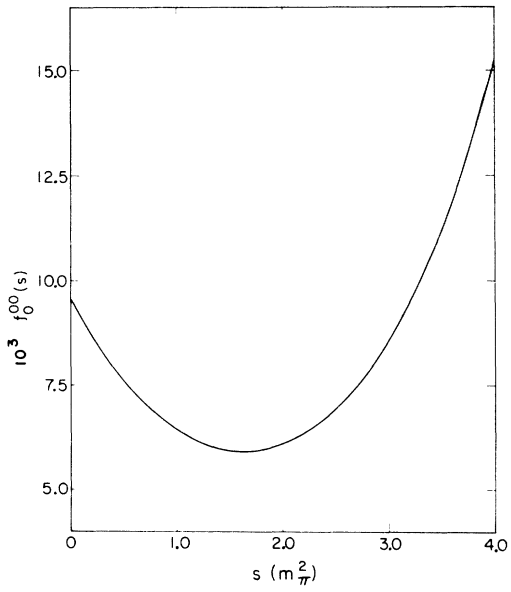

FIG. 7. The $\pi^0\pi^0$ wave $f_0^{00}=\frac{1}{3}(f_0^0+2f_0^2)$ in the unphysical region with the scattering length $a_0^{00}=0.0153$.

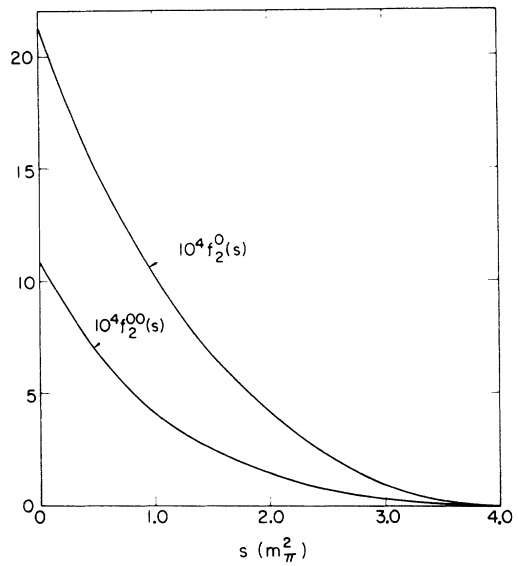

FIG. 8. The d-wave amplitude f_2^0 and the $\pi^0\pi^0$ combination of f_2^{00} in the unphysical region, computed from Eq. (3.1) without error bars.

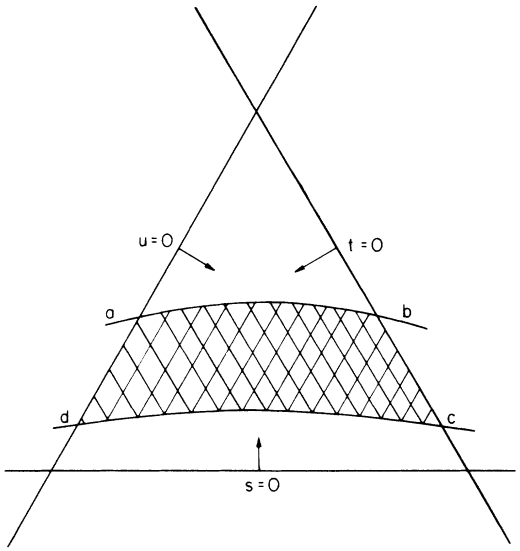

FIG. 9. The $A(s,t,u) = 0$ contour within the Mandelstam triangle lies inside the band shown for all our solutions. The $A = 0$ contour for each individual solution is roughly parallel to the lines ab and cd. The band is defined by the subthreshold partial waves shown in Figs. 5 and 7, together with their uncertainties.

V. DISCUSSION AND CONCLUSIONS

We now briefly compare our results with those of other approaches. First, the data we are considering are in good agreement with the favored "between-down" solution of Morgan and Shaw[26] (at least away from $K\bar{K}$ threshold), which they found using forward dispersion relations. Because of this agreement we find similar values for the s- and p-wave scattering lengths. However, unlike the work of Morgan and Shaw, our analysis is not a prediction but a computation of experimentally determined parameters.

Of the many theoretical models based on combining analyticity, crossing, and unitarity with the experimental p-wave phase shift, our results are closest to those of four recent works. These are models by Widder, by Kühnelt, by Piguet and Wanders,[27] and by Le Guillou, Morel, and Navelet[4] (LGMN). Widder's best solution is the closest, with scattering lengths $a_0^0 = 0.15$, $a_0^2 = -0.064$, and $a_1^1 = 0.037$. The predicted $I = 0$ phase shift, which has $\delta_0^0 = (82 \pm 7)^\circ$ at $s = m_\rho^2$, is in good agreement with our results up to 900 MeV. Below threshold Widder's model has quasilinear s-wave amplitudes with zeros at roughly $s_0 = 1.6$ and $s_2 = 1.12$. Solution A of Kühnelt[27] has an $I = 0$ phase shift which is up to 10° higher than the data in the ρ-mass region. Nonetheless his s- and p-wave scattering lengths and the s-wave zeros are much as we find them to be.

Of the quasilinear models of Piguet and Wanders,[27] which include the ρ as input, that shown in Fig. 12 of their paper gives a δ_0^0 phase shift in good agreement with experiment up to 800 MeV.

The last of the rigorous models we shall mention is that of LGMN.[4] They find values for a_0^0 and $2a_0^0 - 5a_0^2$ larger than ours, and so predict larger values for δ_0^0 than given by the data.[7] However, the ratio $a_0^0 : a_0^2 : a_1^1$ predicted by LGMN is very similar to that we have found. The difference in our results lies in the fact that LGMN obtain a value of $a_1^1 = 0.045$ compared to our value of 0.036. Le Guillou, Morel, and Navelet obtain their result for a_1^1 by fitting the data of Baton *et al.*[8] and extrapolating the fit to threshold. Their larger value for a_1^1 results from the fact that they gave extra weight to the lowest data points (around 500 MeV), and Baton *et al.* have somewhat larger values for δ_1^1 at such energies than given by the data we are considering. For example, at 500 and 525 MeV our computed δ_1^1 values are $(6.3 \pm 0.4)^\circ$ and $(7.6 \pm 0.4)^\circ$, respectively, while Baton has $(8 \pm 5)^\circ$ and $(10 \pm 3)^\circ$. Within the errors, of course, they agree, but since LGMN gave extra weight to these points they find a larger value for a_1^1 than we do.

It is appropriate to remark here that Kühnelt's conclusion,[27] that inelasticity or the passage of δ_0^0 through 180° near 1 GeV does not change the situation in the very-low-energy region by very much, is completely borne out by these comparisons. None of the four theoretical models we have dis-

cussed includes inelasticity or the rapid rise of δ_0^0 through 180° beyond 900 MeV, yet they all have low-energy results in good agreement with the data which do have appreciable inelasticity beyond $K\bar{K}$ threshold and a δ_0^0 which passes through 180°.

All four "rigorous" models we have mentioned are typified by having subthreshold zeros in their s-wave amplitudes and a ρ resonance in their p-wave amplitude. This behavior of the partial waves is in good agreement with the data. Our analysis shows that Weinberg's predictions[3] are also in very good agreement with the data.

This is a very important clue to understanding any dynamical mechanism underlying low-energy $\pi\pi$ scattering. The fact that the Chew-Mandelstam invariant amplitude[28] displays the on-shell appearance of the Adler zero inside the Mandelstam triangle and that this zero continues smoothly into the physical region to become the Legendre zero of the ρ resonance is the first point in unifying all approaches to $\pi\pi$ scattering which give physically reasonable results. Most models which have a p-wave resonating at some mass m_ρ have near-threshold or subthreshold s-wave zeros, and if in the model $m_\rho^2 >> 4$ (as, of course, it is experimentally), quasilinear forms for the partial waves below threshold result. Similarly, quasilinear subthreshold partial waves which have zeros will give a resonating p wave under certain plausible assumptions, such as the hypothesis that "exotic channels are weak."[25]

So far we have only related the Adler zero and the fact that the p wave resonates, without reference either to the particular resonance parameters or to where exactly the Adler zero appears on mass shell inside the Mandelstam triangle. To completely specify the solution to the subthreshold $\pi\pi$ problem we also need the values for a_1^1 and a_0^0/a_0^2. Current algebra determines the s-u odd amplitude at the point $s=u=1$, $t=0$, where two pions are massless. The Adler-Weisberger relation sets the scale in terms of the pion decay constant, f_π. The assumption that the $I=2$ component of the σ commutator vanishes implies that the Chew-Mandelstam invariant amplitude, $A(s,t,u)$, vanishes at $s=t=1$, $u=0$. Now the Adler self-consistency condition means $A(1,1,1)=0$. The PCAC smoothness hypothesis allows us to relate these off-mass-shell conditions to what happens on the plane $s+t+u=4$. If the smoothness of a quasilinear model is assumed then $A(s,t,u)$ must vanish close to the line $s=1$ on mass shell too. What does this mean for the ratio a_0^0/a_0^2? To answer this, the position $s=s_A$ of the zero of the s-wave amplitude, $\frac{1}{3}[f_0^0(s)-f_0^2(s)]$, is a convenient parameter. In an exactly linear model the invariant amplitude A is just this s wave, and so it vanishes on the line $s=s_A$. Now in a quasilinear model the ratio of the s-wave scattering lengths is related to s_A by

$$\frac{a_0^0}{a_0^2} \approx \frac{5}{2} - \frac{6}{s_A} . \tag{5.1}$$

We see if the amplitude were s-wave-dominant, as studied by Chew, Mandelstam, and Noyes,[24] the s wave would have no subthreshold zero (i.e., $s_A=\infty$) and no ρ resonance, and a_0^0/a_0^2 would equal $\frac{5}{2}$. However, nature appears to be more as Weinberg predicted with s_A close to unity; hence a_0^0/a_0^2 is nearer to $-\frac{7}{2}$ than $\frac{5}{2}$. While with reasonable smoothness assumptions this implies that the amplitude vanishes close to the Adler point, we should take care in drawing the conclusion that this also implies that the σ commutator is purely isoscalar. While in an exactly linear model this conclusion would also be true, any additional quadratic and higher-order terms which may be present when we take more than one pion off mass shell may give an unknown value for this commutator, even with s_A close to unity. This is of course a general feature of soft-pion calculations which makes only a linear approximation meaningful.

We have seen why in models utilizing soft-pion results s_A is close to unity. However, from some general principles, other than current algebra, it is not clear why $s_A=1.24$. Namely, what model-independent feature of $\pi\pi$ scattering explains the appearance of the Adler zero on mass shell near the line $s=1.24$? The answer to this question is an unsolved problem.

We now turn to the problem of how the scale of $\pi\pi$ interactions is determined in the various approaches. For this the value of the p-wave scattering length is crucial. Those models which use the experimental p wave as input have their scale given by the ρ mass and width in essentially the ratio Γ_ρ/m_ρ^3, while in current-algebra models, as discussed above, it is the pion-decay constant which sets the scale. The ratio Γ_ρ/m_ρ^3 and the pion-decay constant, f_π, are related by the well-known KSRF relation[12]

$$(a_1^1 \simeq) \frac{1}{24\pi f_\pi^2} \simeq \frac{4m_\rho^2\Gamma_\rho}{(m_\rho^2-4)^{5/2}} . \tag{5.2}$$

We have noted that the on-shell appearance of the Adler zero within the Mandelstam triangle leads to the quasilinearity of the subthreshold s- and p-wave amplitudes and to a value for the ratio $a_0^0 : a_0^2 : a_1^1$ close to that which Weinberg predicts. Further, the fact that the KSRF relation [Eq. (5.2)] is empirically well verified produces the agreement in the values for the s- and p-wave scattering lengths, regardless of whether they are predicted from current-algebra arguments or in some sort

of ρ-dominated model – values which also agree with experiment.[29]

We conclude by recalling what we have achieved. We have shown that the s- and p-wave data of Ref. 7 are consistent with the crossing and analyticity properties used in deriving Roy's equations. In particular the $I=1$ p-wave phase shift, which has very small errors, almost exactly reproduces itself via Roy's equations. For the $I=0$ s wave we have shown the consistency of the favored "down" solution up to 850 MeV. We have computed the s- and p-wave phase shifts in the experimentally unknown region from threshold to 500 MeV. We have also calculated the $l=0,1$, and 2 partial waves below threshold and found the s and p waves to be quasilinear with scattering lengths in agreement with Weinberg's current-algebra predictions and the dispersion-relation results of Morgan and Shaw.

We conclude that current-algebra-based predictions are strongly supported by the data and reiterate an earlier conclusion[6] that the minimum of dynamics necessary to understand low-energy $\pi\pi$ scattering in addition to crossing, elastic unitarity, and analyticity is the on-mass-shell appearance of the Adler zero.

---

*Work supported by the U. S. Atomic Energy Commission.

[1]For general reviews, see J. L. Basdevant, *Springer Tracts in Modern Physics*, edited by G. Höhler (Springer, New York, 1972), Vol. 61, p. 1; J. L. Petersen, Phys. Reports 2C, 155 (1971).

[2]For example, see C. Lovelace, Phys. Letters 28B, 264 (1969).

[3]For example, see S. Weinberg, Phys. Rev. Letters 17, 616 (1966).

[4]For a recent example, see J. C. LeGuillou, A. Morel, and H. Navelet, Nuovo Cimento 5A, 659 (1971).

[5]S. L. Adler, Phys. Rev. 137, B1022 (1965); 139, B1638 (1965).

[6]M. R. Pennington and P. Pond, Nuovo Cimento 3A, 548 (1971).

[7]M. Alston-Garnjost *et al.*, Phys. Letters 36B, 152 (1971); S. M. Flatté *et al.*, Phys. Letters 38B, 232 (1972); S. D. Protopopescu *et al.*, in *Experimental Meson Spectroscopy – 1972*, Proceedings of the Third International Conference, Philadelphia, April 1972, edited by Kwan-Wu Lai and Arthur H. Rosenfeld (A.I.P., New York, 1972).

[8]We should point out that the "down" solution that we use (Ref. 7) tends to be systematically higher by 10° to 15° than Baton's elastic "down" solution in the region of 600–800 MeV. Baillon *et al.* give fewer points (with slightly larger errors) which are in agreement with either set. J. P. Baton, G. Laurens, and J. Reignier, Phys. Letters 33B, 525 (1970); 33B, 528 (1970); P. Baillon *et al.*, *ibid.* 38B, 555 (1972).

[9]S. M. Roy, Phys. Letters 36B, 353 (1971).

[10]J. L. Basdevant, J. C. LeGuillou, and H. Navelet, Nuovo Cimento 7A, 363 (1972).

[11]For general reviews, see A. Martin, Acta Phys. Austr. Suppl. VII, 71 (1970); G. Wanders, *Springer Tracts in Modern Physics*, edited by G. Höhler (Springer, New York, 1971), Vol. 57, p. 22; Lausanne report (lectures given at the Second Seminar on Theoretical Physics organized by GIFT, Madrid), 1971 (unpublished).

[12]K. Kawarabayashi and M. Suzuki, Phys. Rev. Letters 16, 255 (1966); Riazuddin and Fayyazuddin, Phys. Rev. 147, 1071 (1966).

[13]G. Wanders, Helv. Phys. Acta 39, 228 (1966); S. Krinsky, Phys. Rev. D 4, 1046 (1971); J. Dilley and R. Teshima, Nucl. Phys. B46, 275 (1972).

[14]M. R. Pennington, LBL Report No. LBL-918, 1972 (unpublished). There are a number of errors in this paper which will be corrected in a forthcoming revised version.

[15]C. Caso *et al.*, Nuovo Cimento 3A, 287 (1971).

[16]Our definition of the partial-wave amplitudes and of the optical theorem differ by a factor of two from that of LeGuillou *et al.* (Ref. 4). Hence our Eq. (3.12) differs by such a factor from Eq. (IV.14) of Ref. 4.

[17]L. J. Gutay, F. T. Meiere, and J. H. Scharenguivel, Phys. Rev. Letters 23, 431 (1969); D. Cline, K. J. Braun, and V. R. Scherer, Nucl. Phys. B18, 77 (1970).

[18]These results are to be compared with values obtained from other experimental data. T. Maung *et al.* [Phys. Letters 33B, 521 (1970)] obtain $a_0^0 = 0.28 \pm 0.21$. G. Laurens [Ph.D. thesis, University of Paris, CEA Report No. CEA-N-1497 (unpublished)] finds $a_0^2 = -0.055 \pm 0.015$ from a dispersion-relation calculation using the data of Baton *et al.* (Ref. 8) and $a_1^1 = 0.047 \pm 0.003$ by fitting their p-wave data and extrapolating the fit to threshold (cf. Ref. 4). A. Zylberstein *et al.* [Phys. Letters 38B, 457 (1972)] find $a_0^0 = 0.66 \pm 0.17$ from a K_{e4} experiment. *Note added in proof.* Very recent K_{e4} results of E. Beier *et al.* [University of Pennsylvania Report No. UPR-0009E (unpublished)] are in good agreement with our calculated s-wave scattering length; they obtain $0.17 \pm 0.13\,\mu^2$.

[19]Contrary to the implications of R. C. Johnson, [University of Durham report, 1972 (unpublished)], which considers the "up" solution.

[20]P. Basile *et al.*, Phys. Letters 36B, 619 (1971); A. Zylberstein *et al.*, *ibid.* 38B, 457 (1972).

[21]In fact the supplementary crossing conditions first studied by G. Wanders [Nuovo Cimento 63A, 108 (1969)] and R. Roskies [Phys. Rev. D 2, 247; 1649 (1970)] are reasonably well satisfied by our simple Regge and f_0 amplitudes. These conditions are such that a sum of several integrals over physical-region absorptive parts must cancel to give zero. Of course, in practice, they do not exactly cancel. However, we take the ratio of the sum of integrals to the sum of the moduli of these integrals as a convenient measure of this cancellation. Applying this to Eq. (A51) of Ref. 10 we find that with $\sigma_{\text{tot}} = 20$ mb and $b = 6$ (GeV/c)$^{-2}$ this ratio is always of the order of 10^{-5} for all $t, u \in (0,4)$.

[22]A. K. Common and M. K. Pidcock, Nucl. Phys. B42, 194 (1972); P. Grassberger, *ibid.* B42, 461 (1972); A. K. Common, Nuovo Cimento 56A, 524 (1968).
[23]A. Martin, Nuovo Cimento 47A, 265 (1967).
[24]G. F. Chew and S. Mandelstam, Phys. Rev. 119, 467 (1960); G. F. Chew, S. Mandelstam, and H. P. Noyes, *ibid.* 119, 478 (1960).
[25]M. R. Pennington and S. D. Protopopescu, Phys. Letters 40B, 105 (1972); M. R. Pennington and C. Schmid, LBL Report No. LBL-1005, 1972 (unpublished).
[26]D. Morgan and G. Shaw, Phys. Rev. D 2, 520 (1970); D. Morgan, *Springer Tracts in Modern Physics*, edited by G. Höhler (Springer, New York, 1970), Vol. 55, p. 1.
[27]H. Kühnelt, Z. Physik 246, 447 (1971); F. Widder, Acta Phys. Austr. 34, 264 (1971); O. Piguet and G. Wanders, Nucl. Phys. B46, 295 (1972).
[28]This is the most appropriate amplitude for these considerations.
[29]The Lovelace-Veneziano model (Ref. 2) is a particular example of this scheme. The on-mass-shell appearance of the Adler zero is ensured by setting $\alpha_\rho(1) = \frac{1}{2}$, and the scale is determined by the residue of the ρ pole; this means that the s- and p-wave scattering lengths in this model must be close to those given by Weinberg and by the data, which of course they are.

PHYSICAL REVIEW D VOLUME 7, NUMBER 5 1 MARCH 1973

Nuclear Reactions at High Energy*

George W. Barry
Department of Physics, Purdue University, West Lafayette, Indiana 47907
(Received 16 October 1972)

In the quark model, nuclei ($B \leq 2$) have exotic quantum numbers. Given a nuclear reaction in which certain quantum numbers are exchanged, what is the scattering amplitude at high energies, in the GeV region? Does it have Regge behavior? Is it dual? Are there multibaryon resonances? In this context we present a general survey of all high-energy nuclear reactions – mainly those involving light nuclei. For $B = 0$ exchange reactions, like $\pi d \to \pi d$ and $\pi^- h \to \pi^0 t$ ($h \equiv {}^3\mathrm{He}$, $t = {}^3\mathrm{H}$), there is the impulse and rescattering (Glauber) model. For $B = 1$ exchange we discuss the one-pion-exchange (OPE) model for $pp \to d\pi^+$, $pd \to dp$, and $\gamma d \to pn$, and the "knock-on" model for $pd \to \pi^+ t$, $dd \to tp$, $dh \to hd$, $\gamma h \to pd$, and $\gamma\alpha \to pt$. In the case of $B = 2$ exchange we examine the impulse and rescattering diagrams for $\pi d \to d\pi$, $\gamma d \to d\pi^0$, and $\gamma d \to d\gamma$, and use the OPE model to calculate cross sections for $pd \to t\pi$, $pt \to tp$, and $ph \to hp$. Briefly considered are: (1) backward elastic scattering from heavy nuclei ($pA \to Ap$) and (2) inclusive nuclear reactions such as ${}^{14}\mathrm{N} + A \to {}^6\mathrm{Li}$ + anything and $pA \to \bar{d}$ + anything. We postulate that in general nuclear reactions have Regge behavior, but are not dual, because so far there are no exotic multibaryon resonances. Nuclear reactions appear to be completely dominated by anomalous singularities, whereas ordinary nonexotic hadron reactions appear to be dominated by normal singularities and poles.

I. INTRODUCTION

Given a two-body nuclear reaction in which certain quantum numbers are exchanged, what is the differential cross section at high energy, in the GeV region? Forward diffraction scattering has received the lion's share of the attention because the cross sections are large and do not fall off with energy. In this paper, we will be concerned mainly with nondiffractive reactions, those in which quantum numbers are exchanged.

Nuclei are weakly bound systems of protons and neutrons. What is remarkable is that the nucleons retain their identities and do not melt into a multibaryon state bearing no resemblance to its constituents. The general expectation is that nuclear reactions should be completely accountable in terms of the more fundamental nucleon-nucleon interactions. The specific mechanisms are believed to be very complicated and not really worth investigating.

At asymptotic energies the problem might simplify. Let us assume that the scattering amplitude has Regge behavior at high energy. Recall that Regge poles were first introduced into hadron physics as a general prescription for ensuring that unitary bounds on scattering amplitudes are not violated. If only a spin-$J \geq 2$ object is exchanged, the cross section will grow with energy, and thereby violate the Froissart bound. Most of this contribution must therefore be canceled by other high-spin exchanges, and the Regge prescription is the simplest way of ensuring this.

The p-n channel has a bound state, the deuteron.

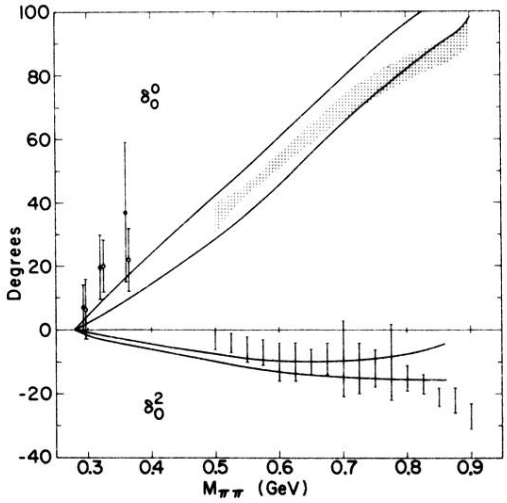

FIG. 4. The $I = 0$ and 2 s-wave phase shifts: The bands bordered by the solid lines are those computed from Eqs. (2.7) and (2.8). The cross-hatched band corresponds to the experimental results for δ_0^0 of Ref. 7, also shown in Fig. 1. The K_{e4} results of Ref. 20 are shown for comparison, where the open circles are the points fixed by their χ^2 fit, and the solid points are those determined by the Pais-Treiman method (Ref. 20). The data points for δ_0^2 are from Baton *et al.* (Ref. 8).